

Asynchronous direct Kalman filtering approach for underwater integrated navigation system

Mohammad Shabani · Asghar Gholami ·
Narjes Davari

Received: 30 December 2013 / Accepted: 6 December 2014 / Published online: 19 December 2014
© Springer Science+Business Media Dordrecht 2014

Abstract This paper presents an asynchronous direct Kalman filter (ADKF) approach for underwater integrated navigation system to improve the performance of the prevalent indirect Kalman filter structure. The designed navigation system is composed of a strapdown inertial navigation system (SDINS) along with Doppler Velocity Log, inclinometer, and depthmeter. In the proposed approach, prediction procedure is placed in the SDINS loop and the correction procedure operates asynchronously out of the SDINS loop. In contrast to the indirect Kalman filter, in the ADKF, the total state such as position, velocity, and orientation are estimated directly within the filter, and further calculations are not performed outside of the filter. This reduces the running time of the computations. To the best of our knowledge, no results have been reported in the literature on the experimental evaluation of a direct Kalman filtering for underwater vehicle navigation. The performance of the designed system is studied using real measurements. The results of the lake test show that the running time of the proposed approach can be improved approximately 7.5 % and also the ADKF exhibits an average

improvement of almost 20 % in position estimate with respect to the prevalent indirect Kalman filter.

Keywords Strapdown inertial navigation system · Underwater integrated navigation system · Kalman filtering

1 Introduction

In many of underwater missions, precise navigation of vehicles is crucial subject. The traditional approach for navigation of the underwater vehicles is Dead Reckoning (DR) [1]. In the two-dimensional DR approach, the current position is calculated, knowing the previous position and measurements of the velocity and heading [2,3]. In underwater navigation, the velocity of the vehicle is measured using Doppler Velocity Log (DVL). The DVL would malfunction under conditions of large roll and pitch [4]. In addition, the low update rate of the DVL (3–7 Hz) and dependency of the DVL signal on the acoustic environment cause the DVL to occasionally be unavailable. The other disadvantage of DR approach arises from the inaccuracy of the velocity data caused by internal biasing errors and external random errors and also error in heading measurement which causes the position error to grow with time due to the transformation of the velocity from instrument frame to navigation frame and time integration of the velocity signal [5,6]. In the strapdown inertial navigation system (SDINS), the principle of

M. Shabani (✉) · A. Gholami · N. Davari
Department of ECE, Isfahan University of Technology,
84156-83111 Isfahan, Iran
e-mail: mohammad.shabani@hotmail.com

A. Gholami
e-mail: gholami@cc.iut.ac.ir

N. Davari
e-mail: n.davari@ec.iut.ac.ir

the DR is used to calculate the vehicles' position [7]. SDINS consists of three orthogonal accelerometers and gyroscopes used to estimate the position, velocity, and orientation of the vehicle [8]. Due to different noise sources in accelerometers and gyroscopes, and the successive time integration of the acceleration, the position error increases exponentially with time [9, 10]. In order to bound the error growth, the SDINS is used together with other navigation aids [11]. In the underwater integrated navigation system, it is common to use the auxiliary sensors such as the DVL, inclinometer, compass, depthmeter, Global Positioning System (GPS), and Acoustic Positioning System (APS) for reducing the position error [12–19]. Unfortunately, the GPS signals are not receivable under the water; hence, the INS/GPS integrated systems for underwater navigation are limited to shallow-water applications where the vehicle must come to the surface regularly to correct its position [20, 21]. One alternative solution for navigation of underwater vehicles is APS, which estimates absolute position of the vehicle, but it requires additional transponders to be either installed at sea floor or mounted to a surface vessel. Since in this approach, vehicle must be placed within the coverage area of transponders, its operation range is restricted. Moreover, the position calibration of the transponders is a difficult time-consuming task, and the installation and maintenance of such a system is expensive [20, 22, 23]. In long period navigation, it is indispensable to use the sensors attached to the body of the vehicle. The favourable sensors for independently underwater navigation used in this paper, consist of the DVL, inclinometer, compass, and depthmeter.

In order to combine the data estimated by SDINS with the signals measured by auxiliary sensors, data fusion methods based on Kalman filtering are used [24–26]. The Kalman filter (KF) [27] is a highly efficient approach for incorporating the noisy measurements to estimate the system state with unpredictable dynamics [28]. In integrated inertial navigation systems, the Kalman filter has been implemented in two approaches, total state space and error state space methods, which, respectively, named as direct and indirect filtering [29, 30].

In the direct filtering, the output of the inertial sensors and the auxiliary measurements are applied to filter and the KF optimally incorporates the inertial data with auxiliary measurements (Fig. 1). One of the major advantages of the direct filtering is that the desired

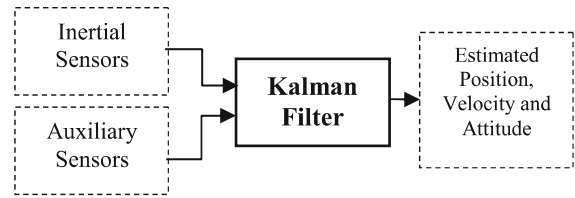


Fig. 1 Direct Kalman filter

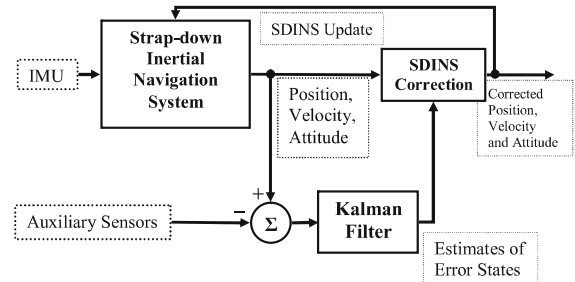


Fig. 2 Indirect Kalman filter

quantity such as position, velocity, and orientation are estimated directly within the filter and further calculations are not performed outside of the filter.

In the indirect Kalman filter, as shown in Fig. 2, difference between SDINS outputs and auxiliary measurements are used by the Kalman filter to estimate the errors of the position, velocity, and orientation. Finally, the SDINS outputs are corrected by the estimated errors. In this structure, the corrected state is feed backed into the SDINS to update it.

To the best of authors' knowledge, this paper reports the first experimental evaluation of a direct Kalman filtering for underwater navigation, where absolute states (i.e., position, velocity, and orientation) are estimated in place of error states. Some reports are found related to GPS/INS integration, where the navigation performance is verified using numerical simulations [31, 32]. In the last decade, the indirect filtering is utilized mostly in underwater integrated navigation systems [13, 17, 18, 22, 33–35]. However, one of the main drawbacks of the indirect structure is that the desired quantities are not estimated directly within the filter, and as shown in Fig. 2, further calculations are required to perform outside of the filter. In this structure, in contrast to position and velocity correction, we cannot easily correct the orientation states. In order to correct the orientation states in the indirect structure, it is necessary to calculate the matrix multiplication and inverse tangent functions [18, 36]. This causes the

computational load of the indirect structure to increase, when compared with the direct structure. The computational load of any Kalman filter structure is relatively high. Therefore, any method that can reduce this problem is worthwhile.

The objective of this paper is to design a direct Kalman filter for underwater integrated navigation system in order to enhance the performance of the current indirect structure. In the proposed approach, the total state of the system is predicted using the system dynamics in the prediction procedure of the Kalman filter. Hence, the prediction procedure is executed with the sampling rate of the inertial sensors. In the correction procedure, on receiving of the auxiliary measurements, the predicted total state is corrected asynchronously. In Sect. 3, we show that due to the direct estimation of the desired quantities within the filter, the computational load of the proposed approach reduces with respect to the prevalent indirect structure. The reduction in the run time of the computations can be very effective in real-time applications.

The structure of this paper is organized as follows. After the introduction, in Sect. 2, ADKF is presented and equations related to this approach are derived. In Sect. 3, the performance of the proposed approach is evaluated using the results of the experimental tests. Finally, conclusions are presented in Sect. 4.

2 Asynchronous direct Kalman filter

In this section, we describe the procedure of the ADKF and derive system and measurement equations for the total states of navigation.

2.1 The system equations

The total state of the system may be included the position, velocity, attitude (roll and pitch), and heading of the vehicle. Since the dynamic equations of the navigation are nonlinear, the general form of a continuous time nonlinear state space model may expressed as [37,38]:

$$\dot{\mathbf{x}} = \mathbf{f}(\mathbf{x}, \mathbf{u}) + \mathbf{G}\mathbf{w}, \mathbf{w} \sim N(\mathbf{0}, \mathbf{Q}_c) \quad (1)$$

where \mathbf{x} is the total state vector of the system which is given as follows:

$$\mathbf{x} = [\mathbf{P}^n, \mathbf{V}^n, \boldsymbol{\Theta}]^T \quad (2)$$

where $\mathbf{P}^n = [L, l, Z]^T$ is the position vector of the vehicle in the navigation frame which is included latitude, longitude, and depth or altitude. $\mathbf{V}^n = [v_N, v_E, v_D]^T$ is the velocity vector resolved in the navigation frame which is included the north velocity, east velocity, and down velocity, and $\boldsymbol{\Theta} = [\phi, \theta, \psi]^T$ is the orientation vector which is composed of the attitude and heading.

\mathbf{f} is the system nonlinear function which describes the dynamic behaviour of the system and is given as follows [4,8]:

$$\dot{\mathbf{P}}^n = \Upsilon \mathbf{V}^n \quad (3)$$

$$\dot{\mathbf{V}}^n = \mathbf{C}_b^n \mathbf{f}^b - (2\boldsymbol{\omega}_{ie}^n + \boldsymbol{\omega}_{en}^n) \times \mathbf{V}^n + \mathbf{g}^n \quad (4)$$

$$\dot{\boldsymbol{\Theta}} = \boldsymbol{\Omega}^{-1} \boldsymbol{\omega}_{nb}^b \quad (5)$$

where

$$\Upsilon = \begin{pmatrix} 1/(R_N + Z) & 0 & 0 \\ 0 & \sec L/(R_E + Z) & 0 \\ 0 & 0 & 1 \end{pmatrix} \quad (6)$$

$$\mathbf{f}^b = [f_x, f_y, f_z]^T \quad (7)$$

$$\boldsymbol{\omega}_{ie}^n = [\Omega \cos L, 0, -\Omega \sin L]^T \quad (8)$$

$$\boldsymbol{\omega}_{en}^n = \left[\frac{v_E}{R_E + Z}, -\frac{v_N}{R_N + Z}, -\frac{v_E \tan L}{R_E + Z} \right]^T \quad (9)$$

$$\mathbf{g}^n = [0, 0, g]^T \quad (10)$$

$$\boldsymbol{\Omega} = \begin{pmatrix} 1 & 0 & -\sin \theta \\ 0 & \cos \phi & \sin \phi \cos \theta \\ 0 & -\sin \phi & \cos \phi \cos \theta \end{pmatrix} \quad (11)$$

$$\begin{aligned} \boldsymbol{\omega}_{nb}^b &= [\omega_x, \omega_y, \omega_z]^T \\ &= \boldsymbol{\omega}_{ib}^b - \mathbf{C}_b^n [\boldsymbol{\omega}_{ie}^n + \boldsymbol{\omega}_{en}^n] \end{aligned} \quad (12)$$

$$R_N = \frac{R(1 - e^2)}{(1 - e^2 \sin^2(L))^{1.5}} \quad (13)$$

$$R_E = \frac{R}{(1 - e^2 \sin^2(L))^{0.5}} \quad (14)$$

The variables R_N , R_E , R , and e represent the meridian radius of curvature, the transverse radius of curvature, the length of the semi-major axis, and the major eccentricity of the ellipsoid of the Earth, respectively [36]. \mathbf{C}_b^n is the transformation matrix from body to navigation axes which may be expressed by Eq. 15, as shown at the top of the next page. \mathbf{f}^b represents the specific force in body axes. $\boldsymbol{\omega}_{ie}^n$ is the angular rate of the Earth expressed in the navigation frame. $\boldsymbol{\omega}_{en}^n$ represents the angular rate of the navigation frame with respect to the Earth-fixed frame. \mathbf{g}^n and g are the gravity vector

in the navigation frame and the Earth gravity constant, respectively. ω_{nb}^b is the angular rate of the vehicle with respect to the navigation frame. $\omega_{ib}^b = [p, q, r]^T$ is the angular rate of the vehicle.

$$\mathbf{C}_b^n = \begin{pmatrix} \cos \theta \cos \psi & -\cos \phi \sin \psi + \sin \phi \sin \theta \cos \psi & \sin \phi \sin \psi + \cos \phi \sin \theta \cos \psi \\ \cos \theta \sin \psi & \cos \phi \cos \psi + \sin \phi \sin \theta \sin \psi & -\sin \phi \cos \psi + \cos \phi \sin \theta \sin \psi \\ -\sin \theta & \sin \phi \cos \theta & \cos \phi \sin \theta \end{pmatrix} \quad (15)$$

The control input \mathbf{u} in Eq. 1 is given by:

$$\mathbf{u} = [\mathbf{f}^b, \omega_{ib}^b] \quad (16)$$

In Eq. 1, \mathbf{w} is process noise due to uncertainty in the control inputs and is modelled in the Kalman filter as a white-noise vector with zero mean and a power spectral density \mathbf{Q}_c , and is called the process noise and may be expressed as follows:

$$\mathbf{w} = [w_{ax}, w_{ay}, w_{az}, w_{gx}, w_{gy}, w_{gz}]^T \quad (17)$$

where $\mathbf{w}_a = [w_{ax}, w_{ay}, w_{az}]^T$ and $\mathbf{w}_g = [w_{gx}, w_{gy}, w_{gz}]^T$ are noise components of accelerometers and gyroscopes, and \mathbf{Q}_c is defined as follows:

$$\mathbf{Q}_c = \text{diag}([q_{ax}, q_{ay}, q_{az}, q_{gx}, q_{gy}, q_{gz}]) \quad (18)$$

where $\mathbf{q}_a = [q_{ax}, q_{ay}, q_{az}]^T$ and $\mathbf{q}_g = [q_{gx}, q_{gy}, q_{gz}]^T$ are the spectral density of the signals measured by accelerometers and gyroscopes.

2.2 The measurement equations

In this section, in order to derive the measurement model, all possible measurements used in underwater navigation, including the position, velocity, attitude, and heading, are considered. In the proposed approach, the measurements of the system are a nonlinear combination of the states which are corrupted with noise. This can be given in terms of the total states of the system by the following equation:

$$\mathbf{y} = \mathbf{h}(\mathbf{x}) + \mathbf{v}, \mathbf{v} \sim N(\mathbf{0}, \mathbf{R}) \quad (19)$$

where \mathbf{y} is the measurement vector of the system which is defined as follows:

$$\mathbf{y} = [\mathbf{P}_m^n, \mathbf{V}_m^b, \Theta_m]^T \quad (20)$$

where $\mathbf{P}_m^n = [L_m, l_m, Z_m]^T$ is the auxiliary signals of the position measured by the GPS and depthmeter which are included latitude, longitude, and

depth or altitude. $\mathbf{V}_m^b = [v_x, v_y, v_z]^T$ is the measurements of the DVL in the instrument frame, and $\Theta_m = [\phi_m, \theta_m, \psi_m]^T$ is the auxiliary signals of ori-

entation. The attitude measurements is computed by the accelerometer signals, and heading measurement is provided by a compass.

\mathbf{h} , in Eq. 19, is the measurement model function, and \mathbf{v} represents the measurement noise which is assumed to be a zero mean, Gaussian white-noise process with known covariance matrix \mathbf{R} .

The latitude and longitude measurements can be expressed in terms of the states of the horizontal position by the following equations:

$$\begin{aligned} L_m &= L + v_L \\ l_m &= l + v_l \end{aligned} \quad (21)$$

The measurement output matrix and measurement noise matrix for the horizontal position may be given by:

$$\mathbf{H}_{\text{gps}} = \begin{pmatrix} 1 & 0 & 0 & 0 & 0 & 0 & 0 & 0 & 0 \\ 0 & 1 & 0 & 0 & 0 & 0 & 0 & 0 & 0 \end{pmatrix} \quad (22)$$

$$\mathbf{R}_{\text{gps}} = \begin{pmatrix} \sigma_L^2 & 0 \\ 0 & \sigma_l^2 \end{pmatrix} \quad (23)$$

where σ_L^2 and σ_l^2 are the variance of the measurements of the latitude and longitude, respectively.

The measurement equation of the depthmeter is defined by:

$$Z_m = Z + v_z \quad (24)$$

The matrices of \mathbf{H} and \mathbf{R} for the depthmeter may be given as follows:

$$\mathbf{H}_z = (0 \ 0 \ 1 \ 0 \ 0 \ 0 \ 0 \ 0 \ 0) \quad (25)$$

$$\mathbf{R}_z = (\sigma_z^2) \quad (26)$$

where σ_z^2 is the variance of the depthmeter's measurement.

The relationship between the DVL's measurements and the states of the velocity may be expressed by the following nonlinear equation:

$$\mathbf{V}_m^b = \mathbf{C}_n^b \mathbf{V}^n + v_v \quad (27)$$

This equation can be expressed in component form as follows:

$$v_x = C_{11}v_N + C_{21}v_E + C_{31}v_D + v_{v_x} \quad (28)$$

$$v_y = C_{12}v_N + C_{22}v_E + C_{32}v_D + v_{v_y} \quad (29)$$

$$v_z = C_{13}v_N + C_{23}v_E + C_{33}v_D + v_{v_z} \quad (30)$$

where C_{ij} is the element in the i th row and the j th column of the transformation matrix from body frame to navigation frame (i.e., \mathbf{C}_b^n).

The measurement output matrix for the DVL may be given by:

$$\begin{aligned} \mathbf{H}_{\text{dvl}} &= \left. \frac{\partial \mathbf{V}_m^b}{\partial \mathbf{x}_i} \right|_{\hat{\mathbf{x}}(t_k)} \\ &= \begin{pmatrix} 0 & 0 & 0 & C_{11} & C_{21} & C_{31} & H_{17} & H_{18} & H_{19} \\ 0 & 0 & 0 & C_{12} & C_{22} & C_{32} & H_{27} & H_{28} & H_{29} \\ 0 & 0 & 0 & C_{13} & C_{23} & C_{33} & H_{37} & H_{38} & H_{39} \end{pmatrix} \end{aligned} \quad (31)$$

The other components of the matrix \mathbf{H}_{dvl} , H_{ij} are given in the appendix. The measurement noise matrix of the DVL measurements may be expressed as follows:

$$\mathbf{R}_{\text{dvl}} = \begin{pmatrix} \sigma_{v_x}^2 & 0 & 0 \\ 0 & \sigma_{v_y}^2 & 0 \\ 0 & 0 & \sigma_{v_z}^2 \end{pmatrix} \quad (32)$$

where $\sigma_{v_x}^2$, $\sigma_{v_y}^2$, and $\sigma_{v_z}^2$ are the variance of the DVL's measurements.

The measurement model of attitude may be given by:

$$\begin{aligned} \phi_m &= \phi + v_\phi \\ \theta_m &= \theta + v_\theta \end{aligned} \quad (33)$$

where ϕ_m and θ_m are the auxiliary signals of roll and pitch computed from the supplementary accelerometer's signals. Under circumstances that the vehicle moves at a constant velocity, the only acceleration acting on the vehicle is the acceleration due to gravity. Therefore, the roll and pitch signals may be computed by the following equations:

$$\theta_m = \frac{\sin^{-1}(f_{sx})}{g} \quad (34)$$

$$\phi_m = -\frac{\sin^{-1}(f_{sy})}{g \cos(\theta)} \quad (35)$$

where f_{sx} and f_{sy} are the accelerations acting on the vehicle along the forward and starboard measured by the supplementary accelerometers. The gravity g is computed by the following equation [36]:

$$g = \frac{g_0}{1 + Z/R_0} \quad (36)$$

where

$$g_0 = 9.780318 \times (1 + 5.3024 \times 10^{-3} \sin^2 L - 5.9 \times 10^{-6} \sin^2 2L) \quad (37)$$

$$R_0 = \sqrt{R_N R_E} \quad (38)$$

The measurement matrices for the signals of the roll and pitch may be given by:

$$\mathbf{H}_\theta = \begin{pmatrix} 0 & 0 & 0 & 0 & 0 & 0 & 1 & 0 & 0 \\ 0 & 0 & 0 & 0 & 0 & 0 & 0 & 1 & 0 \end{pmatrix} \quad (39)$$

$$\mathbf{R}_\theta = \begin{pmatrix} \sigma_\phi^2 & 0 \\ 0 & \sigma_\theta^2 \end{pmatrix} \quad (40)$$

where σ_ϕ^2 and σ_θ^2 are the variance of the signals of the roll and pitch, respectively.

The measurement equation of the compass is defined by:

$$\psi_m = \psi + v_\psi \quad (41)$$

The measurement matrices of the compass may be given as follows:

$$\mathbf{H}_\psi = (0 \ 0 \ 0 \ 0 \ 0 \ 0 \ 0 \ 0 \ 1) \quad (42)$$

$$\mathbf{R}_\psi = (\sigma_\psi^2) \quad (43)$$

where σ_ψ^2 is the variance of the compass's measurement.

2.3 The asynchronous integration

In order to formulate the Kalman filter, Eqs. (1) and (19) are required. In this section, the equations for constructing the ADKF are derived and the procedures for executing these equations is described.

The prediction procedure In the prediction procedure, the total state of the system $\hat{\mathbf{x}}^-$ and covariance of the state \mathbf{P}^- are predicted. For each time step of inertial sensors, prediction procedure evaluates the Jacobian matrices of the system equation, \mathbf{F} and \mathbf{G} and matrix \mathbf{Q}_c ; computes the discretized matrices \mathbf{A} and \mathbf{Q} ; predicts the total state of the navigation system and its covariance. The elements of the Jacobian matrices of

the system equation \mathbf{f} at time step t_k are computed as follows:

$$\mathbf{F}(t_k) = \left. \frac{\partial f_i}{\partial x_i} \right|_{\hat{\mathbf{x}}(t_k)}, \quad \mathbf{G}(t_k) = \left. \frac{\partial f_i}{\partial w_i} \right|_{\hat{\mathbf{x}}(t_k)}, \quad i = 1, \dots, 9 \quad (44)$$

where x_i s and w_i s are the elements of the total state of the system \mathbf{x} and the white-noise vector \mathbf{w} , as shown in Eqs. (2) and (17), respectively.

In order to execute the prediction procedure, the system equations can be expressed in component form as follows:

$$f_1 = \dot{L} = \frac{v_N}{R_N + Z} \quad (45)$$

$$f_2 = \dot{l} = \frac{v_E \sec(L)}{R_E + Z} \quad (46)$$

$$f_3 = \dot{Z} = v_D \quad (47)$$

$$f_4 = \dot{v}_N = f_N - v_E (2\Omega + \dot{l}) \sin(L) + v_D \dot{L} \quad (48)$$

$$f_5 = \dot{v}_E = f_E + (2\Omega + \dot{l}) (v_N \sin(L) + v_D \cos(L)) \quad (49)$$

$$f_6 = \dot{v}_D = f_D - v_E (2\Omega + \dot{l}) \cos(L) + v_N \dot{L} + g \quad (50)$$

$$f_7 = \dot{\phi} = (\omega_y \sin \phi + \omega_z \cos \phi) \tan \theta + \omega_x \quad (51)$$

$$f_8 = \dot{\theta} = (\omega_y \cos \phi - \omega_z \sin \phi) \quad (52)$$

$$f_9 = \dot{\psi} = (\omega_y \sin \phi + \omega_z \cos \phi) \sec \theta \quad (53)$$

where

$$f_N = C_{11}(f_x + w_1) + C_{12}(f_y + w_2) + C_{13}(f_z + w_3) \quad (54)$$

$$f_E = C_{21}(f_x + w_1) + C_{22}(f_y + w_2) + C_{23}(f_z + w_3) \quad (55)$$

$$f_D = C_{31}(f_x + w_1) + C_{32}(f_y + w_2) + C_{33}(f_z + w_3) \quad (56)$$

$$\omega_x = (P + w_4) - (C_{11}\omega_N + C_{21}\omega_E + C_{31}\omega_D) \quad (57)$$

$$\omega_y = (q + w_5) - (C_{12}\omega_N + C_{22}\omega_E + C_{32}\omega_D) \quad (58)$$

$$\omega_z = (r + w_6) - (C_{13}\omega_N + C_{23}\omega_E + C_{33}\omega_D) \quad (59)$$

$$\omega_N = \Omega \cos L + \frac{v_E}{R_E + Z} \quad (60)$$

$$\omega_E = -\frac{v_N}{R_N + Z} \quad (61)$$

$$\omega_D = -\Omega \sin L - \frac{v_E \tan L}{R_E + Z} \quad (62)$$

where Ω is the Earth's rate, and C_{ij} is the element in the i th row and the j th column of the transformation matrix which is given by Eq. (15).

By differentiating Eqs. (45)–(53) according to Eq. (44), the matrices \mathbf{F} and \mathbf{G} are calculated. Further details for the derivatives in the matrices \mathbf{F} and \mathbf{G} are presented in the appendix.

The discretized matrices \mathbf{A} and \mathbf{Q} at time step t_k are computed as follows [29]:

$$\mathbf{A}(t_k) = \exp(\mathbf{F}dt) \quad (63)$$

$$\mathbf{Q}(t_k) = \frac{1}{2} \left[\mathbf{A}(t_k) \mathbf{G} \mathbf{Q}_c \mathbf{G}^T \mathbf{A}^T(t_k) + \mathbf{G} \mathbf{Q}_c \mathbf{G}^T \right] dt \quad (64)$$

where $dt = t_k - t_{k-1}$ is the sampling time of inertial sensors.

The navigation state and its covariance are predicted by the following equations:

$$\hat{\mathbf{x}}^-(t_k) = \int_{t_{k-1}}^{t_k} \mathbf{f}(\hat{\mathbf{x}}^+(t_{k-1}), \mathbf{u}(t_{k-1}), 0) dt \quad (65)$$

$$\mathbf{P}^-(t_k) = \mathbf{A}(t_{k-1}) \mathbf{P}^+(t_{k-1}) \mathbf{A}^T(t_{k-1}) + \mathbf{Q}(t_{k-1}) \quad (66)$$

The prediction of the navigation state is performed via the rectangular integration [37]:

$$\Delta \mathbf{x} = \mathbf{f}(\hat{\mathbf{x}}^+(t_{k-1}), \mathbf{u}(t_{k-1}), 0) dt$$

$$\hat{\mathbf{x}}^-(t_k) = \hat{\mathbf{x}}^+(t_{k-1}) + \Delta \mathbf{x} \quad (67)$$

The correction procedure Since auxiliary sensors operate with different sampling frequency, the correction procedure is executed asynchronously. Operating in asynchronous mode means that when one or more of the auxiliary sensors are received at time t_k , the correction parameters associated with those sensors [i.e., $\mathbf{y}(t_k)$, $\mathbf{H}(t_k)$, and $\mathbf{R}(t_k)$] are formed, and then the correction equations of the KF are executed. In the event that none of the auxiliary sensors are available, the correction procedure will not be executed. In this case, the filter continues to operate without correction using the prediction procedure. The total state of the navigation and its covariance matrix is predicted with sampling frequency of inertial sensors according to Eqs. (65)–(67) with or without the correction procedure. On receiving of a new auxiliary signal $\mathbf{y}(t_k)$, the navigation state \mathbf{x}^+ and its associated covariance matrix \mathbf{P}^+ at time step t_k are corrected by the following equation:

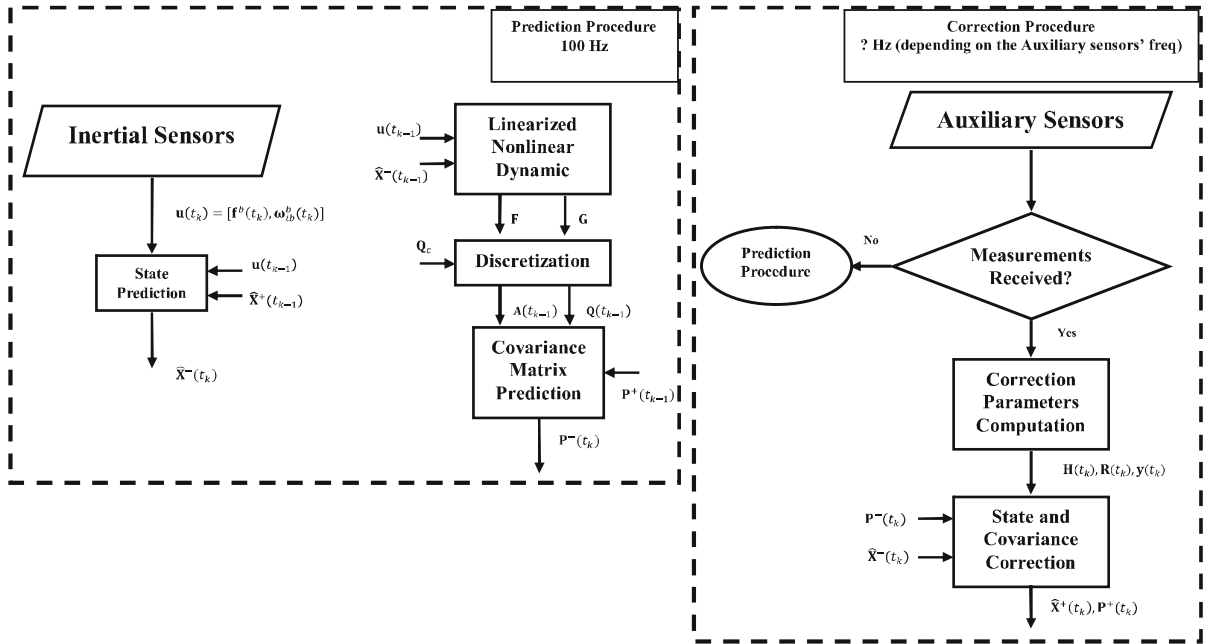


Fig. 3 Asynchronous direct Kalman filter for underwater navigation

Fig. 4 Instrumented vessel for experiments



$$\mathbf{K}(t_k) = \mathbf{P}^-(t_k) \mathbf{H}^T(t_k) \times \left(\mathbf{H}(t_k) \mathbf{P}^-(t_k) \mathbf{H}^T(t_k) + \mathbf{R}(t_k) \right)^{-1} \quad (68)$$

$$\hat{\mathbf{x}}^+(t_k) = \hat{\mathbf{x}}^-(t_k) + \mathbf{K}(t_k) \times (\mathbf{y}(t_k) - \mathbf{H}(t_k) \hat{\mathbf{x}}^-(t_k)) \quad (69)$$

$$\mathbf{P}^+(t_k) = (\mathbf{I} - \mathbf{K}(t_k) \mathbf{H}(t_k)) \mathbf{P}^-(t_k) \quad (70)$$

where $\mathbf{K}(t_k)$ is the Kalman gain matrix, and \mathbf{I} is the identity matrix. In the best case, which all of the auxiliary sensors are available, the matrices \mathbf{H} and \mathbf{R} are given by the Eq. (71). The dimensions of the

correction parameters are determined based on the number of received auxiliary sensors. When one of the sensors isn't received, the matrices associated with that sensor, which was given in Sect. 2, are removed from the correction parameters. The flowchart of the ADKF is illustrated in Fig. 3.

$$\mathbf{H} = \begin{pmatrix} 1 & 0 & 0 & 0 & 0 & 0 & 0 & 0 & 0 \\ 0 & 1 & 0 & 0 & 0 & 0 & 0 & 0 & 0 \\ 0 & 0 & 1 & 0 & 0 & 0 & 0 & 0 & 0 \\ 0 & 0 & 0 & C_{11} & C_{21} & C_{31} & H_{17} & H_{18} & H_{19} \\ 0 & 0 & 0 & C_{12} & C_{22} & C_{32} & H_{27} & H_{28} & H_{29} \\ 0 & 0 & 0 & C_{13} & C_{23} & C_{33} & H_{37} & H_{38} & H_{39} \\ 0 & 0 & 0 & 0 & 0 & 0 & 1 & 0 & 0 \\ 0 & 0 & 0 & 0 & 0 & 0 & 0 & 1 & 0 \\ 0 & 0 & 0 & 0 & 0 & 0 & 0 & 0 & 1 \end{pmatrix},$$

$$\mathbf{R} = \begin{pmatrix} \sigma_L^2 & 0 & 0 & 0 & 0 & 0 & 0 & 0 & 0 \\ 0 & \sigma_I^2 & 0 & 0 & 0 & 0 & 0 & 0 & 0 \\ 0 & 0 & \sigma_z^2 & 0 & 0 & 0 & 0 & 0 & 0 \\ 0 & 0 & 0 & \sigma_{v_x}^2 & 0 & 0 & 0 & 0 & 0 \\ 0 & 0 & 0 & 0 & \sigma_{v_y}^2 & 0 & 0 & 0 & 0 \\ 0 & 0 & 0 & 0 & 0 & \sigma_{v_z}^2 & 0 & 0 & 0 \\ 0 & 0 & 0 & 0 & 0 & 0 & \sigma_\phi^2 & 0 & 0 \\ 0 & 0 & 0 & 0 & 0 & 0 & 0 & \sigma_\theta^2 & 0 \\ 0 & 0 & 0 & 0 & 0 & 0 & 0 & 0 & \sigma_\psi^2 \end{pmatrix} \quad (71)$$

3 Experimental results

The lake test was carried out on February 26, 2013 in Zobahan Lake, Isfahan Province. As shown in Fig. 4, experiments were performed using an instrumented vessel. A fibre-optic gyro IMU, a DVL, and a GPS receiver were mounted on the vessel, as depicted in Fig. 5. In addition to primary accelerometers used in the SDINS, the supplementary orthogonal triad of the accelerometers was used for computing the auxiliary attitude signals. The estimated position is assessed with respect to a reference trajectory made by the smoothed best estimate of the GPS data. In order to hold the DVL beneath the water, a stand was also utilized. The technical specifications of the instruments are shown in Table 1.

Several lake test trajectories were carried out using the setup described earlier. Two trajectories will be presented in this paper to show the performance of the ADKF. The vessel carries an industrial PC to log the outputs of all navigation sensors during the mission; then, offline post-processing is performed. To validate the performance of the ADKF, the indirect KF (IKF) (Fig. 2) is also implemented according to [17, 18] and their results are compared with those of the ADKF. The implementation details of the IKF were given in [39].

Fig. 5 Instruments mounted on the vessel

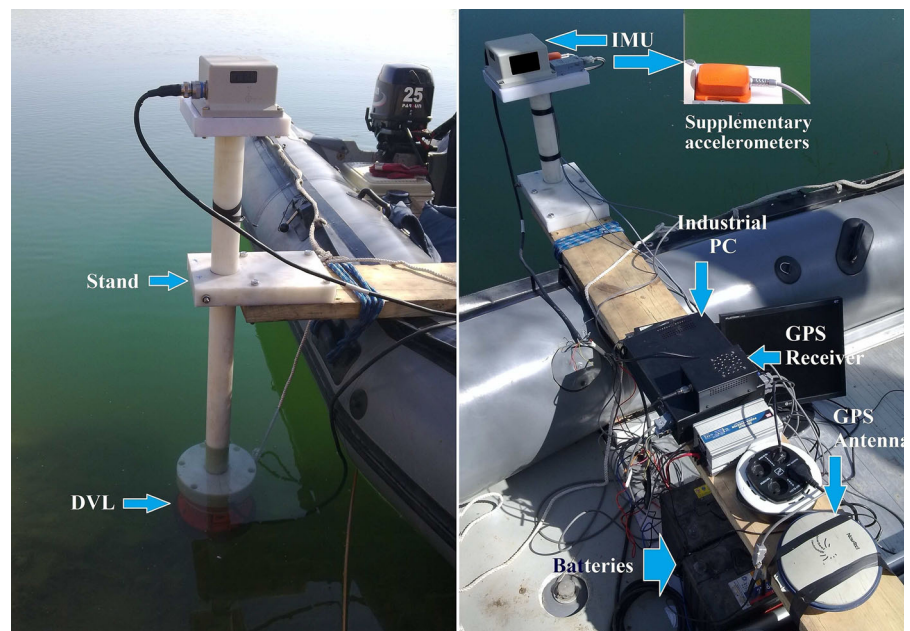
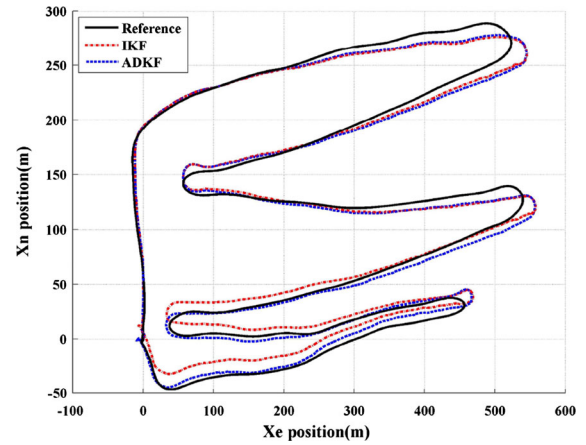
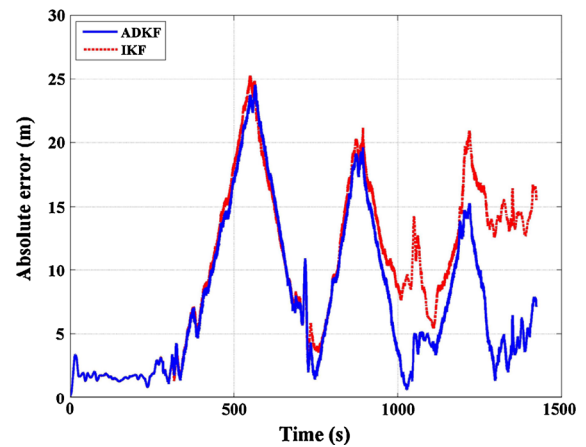


Table 1 The technical specifications of the instruments

Gyroscope	
Bias offset	± 20 deg/h
Bias stability	1 deg/h @ 1σ
Angular random walk	0.0667 deg/h @ 1σ
Bandwidth	50 Hz
Data rate	100 Hz
Accelerometer	
Bias offset	± 50 mg
In run bias variation	0.25 mg @ 1σ
Output Noise	$55 \mu\text{g}/\sqrt{\text{Hz}}$ @ 1σ
Bandwidth	50 Hz
Data rate	100 Hz
DVL	
Frequency	300 kHz
Accuracy	$1\% \pm 2 \text{ mm/s}$ @ 1σ
Maximum altitude	300 m
Minimum altitude	0.6 m
Maximum velocity	± 20 knots
Maximum ping rate	3/s knots
GPS	
Position accuracy	< 2 m
Data rate	5 Hz
Supplementary accelerometer	
Bias stability	0.02 m/s^2 @ 1σ
Noise	$0.002 \text{ m/s}^2/\sqrt{\text{Hz}}$
Bandwidth	30 Hz
Data rate	100 Hz

Figure 6 shows the position estimated in the directions of the east and north by the ADKF and the IKF approaches when travelling the trajectory No. 1. In Fig. 7, curves of the absolute error are shown. Absolute error is defined as the magnitude of the difference between the reference trajectory provided by the GPS and the position estimated by the approaches. According to these figures, the positions estimated by both approaches follow the reference trajectory with a bounded error. The estimation error in two approaches is increased due to the uncompensated residual errors caused by the sensors, although the rate of the error growth of the ADKF is less than the IKF.

**Fig. 6** Estimated positions by the ADKF and feedback indirect KF in first trajectory**Fig. 7** Absolute error of the estimated position in first trajectory

To compare quantitatively the performance of the ADKF and IKF approaches, the root mean square error (RMSE) criterion and relative error is used as follows:

$$\text{SE} = (R_x - E_x)^2 + (R_y - E_y)^2 + (R_z - E_z)^2$$

$$\text{RMSE} = \sqrt{\text{mean}(\text{SE})} \quad (72)$$

$$\text{Relative RMSE} = \frac{\text{RMSE}}{\text{Travelled Distance}} \times 100 \quad (73)$$

where R_i and E_i are the reference and estimated position along the axis i .

In the test related to the trajectory No. 1 where the vessel travelled approximately 3,213 m for nearly 24 min, the RMSEs of the position estimated by the ADKF and IKF are 9.81 and 11.88 m and relative errors

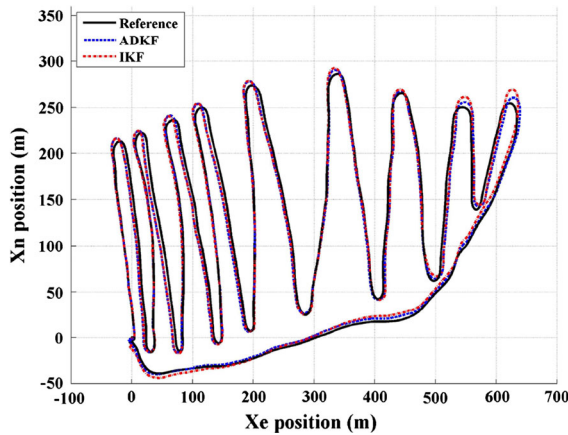


Fig. 8 Estimated positions by the ADKF and feedback indirect KF in second trajectory

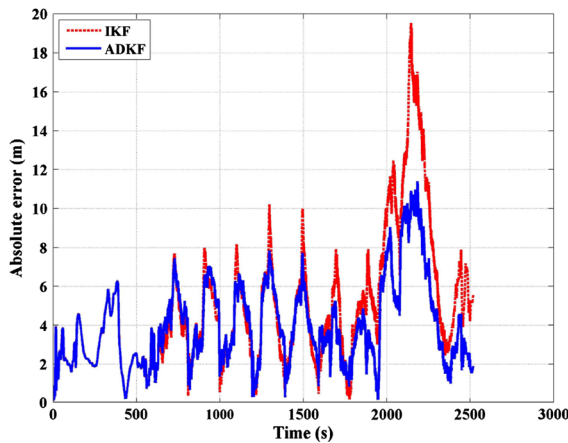


Fig. 9 Absolute error of the estimated position in second trajectory

are 0.31 and 0.37 % of the travelled distance, respectively. In order to validate the computational load of the ADKF, the offline running times of the approaches are compared. In this test, the ADKF and IKF take 2 min and 50 s and 3 min and 3 s, respectively. Therefore, the ADKF estimates the output state more accurately and faster than the IKF.

Table 2 Performance comparison between ADKF and IKF

Trajectory	Distance/time	Approach	RMSE(m)	Relative RMSE (%)	Running time
First trajectory	3,213 m 24 min	ADKF	9.81	0.31	2 min 50 s
		IKF	11.88	0.37	3 min 3 s
Second trajectory	4,897 m 42 min	ADKF	4.52	0.092	5 min 4 s
		IKF	5.86	0.12	5 min 30 s

In Fig. 8, the position estimated by the approaches in the directions of the east and north are compared when travelling the second trajectory, and Figure 9 shows the absolute error curves for this trajectory.

In the test related to the trajectory No. 2 where the vessel travelled approximately 4,897 m for nearly 42 min, the RMSEs of the position estimated by the ADKF and IKF are 4.52 and 5.86 m and relative errors are 0.092 and 0.12 % of the travelled distance, respectively. The running time of the ADKF and IKF is 5 min and 4 s and 5 min and 30 s, respectively. Therefore, according to the results obtained from the second test, the results of the first test are confirmed. The results obtained from the practical test for travelled trajectories are summarized in Table 2.

4 Conclusions

In the underwater integrated navigation systems, it is usually to use the indirect Kalman filter. However, one of the major drawbacks of the indirect structure is that the desired quantities are not estimated directly within the filter, and further calculations are required to perform outside of the filter. In this structure, unlike the position and velocity correction, the orientation states cannot be simply corrected. Due to the matrix multiplication operation and inverse tangent computation for correcting the orientation states, the computational load of indirect structure increases compared with the direct structure. In this paper, we have presented an asynchronous direct Kalman filtering approach, called the ADKF, for underwater integrated navigation system to improve the performance of the prevalent indirect structure. By asynchronously implementing the direct Kalman filter, the prediction procedure is placed in the SDINS loop and the correction procedure operates asynchronously out of the SDINS loop. In the proposed approach, the desired quantities are estimated directly within the filter and further calculations are not

performed outside of the filter. Hence, the running time of the computations is reduced with respect to the prevalent indirect structure. The results of the lake test show that the running time of the proposed approach can be improved approximately 7.5% and also the ADKF exhibits an average improvement of almost 20% in position estimate with respect to the prevalent indirect Kalman filter.

Acknowledgments The authors would like to thank Mehdi Emami for his help in the experiments, and the anonymous reviewers for providing valuable comments to improve this paper.

Appendix: The derivatives in the Jacobian matrices \mathbf{F} , \mathbf{G} , and \mathbf{H}_{dvl}

The matrices \mathbf{F} and \mathbf{G} are formed according to the matrices at the top of the next page.

The derivatives in the Jacobian matrix \mathbf{F} are given by

$$\mathbf{F} = \begin{pmatrix} F_{11} & 0 & F_{13} & F_{14} & 0 & 0 & 0 & 0 & 0 \\ F_{21} & 0 & F_{23} & 0 & F_{25} & 0 & 0 & 0 & 0 \\ 0 & 0 & 0 & 0 & 0 & F_{36} & 0 & 0 & 0 \\ F_{41} & 0 & F_{43} & F_{44} & F_{45} & F_{46} & F_{47} & F_{48} & F_{49} \\ F_{51} & 0 & F_{53} & F_{54} & F_{55} & F_{56} & F_{57} & F_{58} & F_{59} \\ F_{61} & 0 & F_{63} & F_{64} & F_{65} & 0 & F_{67} & F_{68} & F_{69} \\ F_{71} & 0 & F_{73} & F_{74} & F_{75} & F_{76} & F_{77} & F_{78} & F_{79} \\ F_{81} & 0 & F_{83} & F_{84} & F_{85} & F_{86} & F_{87} & F_{88} & F_{89} \\ F_{91} & 0 & F_{93} & F_{94} & F_{95} & F_{96} & F_{97} & F_{98} & F_{99} \end{pmatrix},$$

$$\mathbf{G} = \begin{pmatrix} 0 & 0 & 0 & 0 & 0 & 0 \\ 0 & 0 & 0 & 0 & 0 & 0 \\ 0 & 0 & 0 & 0 & 0 & 0 \\ C_{11} & C_{12} & C_{13} & 0 & 0 & 0 \\ C_{21} & C_{22} & C_{23} & 0 & 0 & 0 \\ C_{31} & C_{32} & C_{33} & 0 & 0 & 0 \\ 0 & 0 & 0 & 1 & \sin \phi \tan \theta & \cos \phi \tan \theta \\ 0 & 0 & 0 & 0 & \cos \phi & -\sin \phi \\ 0 & 0 & 0 & 0 & \sin \phi \sec \theta & \cos \phi \sec \theta \end{pmatrix}$$

$$F_{11} = \frac{\partial f_1}{\partial L} = -\frac{\partial R_N}{\partial L} \frac{v_N}{R_N + Z}$$

$$F_{13} = \frac{\partial f_1}{\partial Z} = -\frac{v_N}{(R_N + Z)^2}$$

$$F_{14} = \frac{\partial f_1}{\partial v_N} = \frac{1}{R_N + Z}$$

$$F_{21} = \frac{\partial f_2}{\partial L} = v_E \left[\frac{\sec L \tan L}{R_E + Z} + \frac{-\partial R_N}{\partial L} \frac{\sec L}{(R_E + Z)^2} \right]$$

$$F_{23} = \frac{\partial f_2}{\partial Z} = -\frac{v_E \sec L}{(R_E + Z)^2}$$

$$F_{25} = \frac{\partial f_2}{\partial v_E} = \frac{\sec L}{R_E + Z}$$

$$F_{36} = \frac{\partial f_3}{\partial v_D} = 1$$

$$F_{41} = \frac{\partial f_4}{\partial L} = -v_E \left[\frac{\partial f_2}{\partial L} \sin L + \frac{v_E}{R_E + Z} \right] + v_D \frac{\partial f_1}{\partial L}$$

$$F_{43} = \frac{\partial f_4}{\partial Z} = -v_E \left(\sin L \frac{\partial f_2}{\partial Z} \right) + v_D \frac{\partial f_1}{\partial Z}$$

$$F_{44} = \frac{\partial f_4}{\partial v_N} = v_D \frac{\partial f_1}{\partial v_N}$$

$$F_{45} = \frac{\partial f_4}{\partial v_E} = -2\Omega \sin L - \frac{2v_E \tan l}{R_E + Z}$$

$$F_{46} = \frac{\partial f_4}{\partial v_D} = \frac{v_N}{R_N + Z}$$

$$F_{47} = \frac{\partial f_4}{\partial \phi} = \frac{\partial C_{11}}{\partial \phi} f_x + \frac{\partial C_{12}}{\partial \phi} f_y + \frac{\partial C_{13}}{\partial \phi} f_z$$

and

$$F_{48} = \frac{\partial f_4}{\partial \theta} = \frac{\partial C_{11}}{\partial \theta} f_x + \frac{\partial C_{12}}{\partial \theta} f_y + \frac{\partial C_{13}}{\partial \theta} f_z$$

$$F_{49} = \frac{\partial f_4}{\partial \psi} = \frac{\partial C_{11}}{\partial \psi} f_x + \frac{\partial C_{12}}{\partial \psi} f_y + \frac{\partial C_{13}}{\partial \psi} f_z$$

$$F_{51} = \frac{\partial f_5}{\partial L} = v_N \left[2\Omega \cos L + \frac{\partial f_2}{\partial L} \sin L + \frac{v_E \tan L}{R_E + Z} \right] + v_D \left[-2\Omega \sin L + \frac{\partial f_2}{\partial L} \cos L + \frac{v_E}{R_E + Z} \right]$$

$$F_{53} = \frac{\partial f_5}{\partial Z} = \frac{\partial f_2}{\partial Z} (v_N \sin L + v_D \cos L)$$

$$F_{54} = \frac{\partial f_5}{\partial v_N} = \left(2\Omega + \frac{v_E \sec L}{R_E + Z} \right) \sin L$$

$$F_{55} = \frac{\partial f_5}{\partial v_E} = \frac{v_D + v_N \tan L}{R_E + Z}$$

$$F_{56} = \frac{\partial f_5}{\partial v_D} = 2\Omega \cos L + \frac{v_E}{R_E + Z}$$

$$F_{57} = \frac{\partial f_5}{\partial \phi} = \frac{\partial C_{21}}{\partial \phi} f_x + \frac{\partial C_{22}}{\partial \phi} f_y + \frac{\partial C_{23}}{\partial \phi} f_z$$

$$F_{58} = \frac{\partial f_5}{\partial \theta} = \frac{\partial C_{21}}{\partial \theta} f_x + \frac{\partial C_{22}}{\partial \theta} f_y + \frac{\partial C_{23}}{\partial \theta} f_z$$

$$F_{59} = \frac{\partial f_5}{\partial \psi} = \frac{\partial C_{21}}{\partial \psi} f_x + \frac{\partial C_{22}}{\partial \psi} f_y + \frac{\partial C_{23}}{\partial \psi} f_z$$

$$\begin{aligned}
F_{61} &= \frac{\partial f_6}{\partial L} = -v_E \left[-2\Omega \sin L + \frac{\partial f_2}{\partial L} \cos L \right] \\
&\quad - v_E \left[\frac{v_E \tan L}{R_E + Z} \right] - v_N \frac{\partial f_1}{\partial L} \\
F_{63} &= \frac{\partial f_6}{\partial Z} = -v_E \cos L \frac{\partial f_2}{\partial Z} - v_N \frac{\partial f_1}{\partial Z} \\
F_{64} &= \frac{\partial f_6}{\partial v_N} = \frac{-2v_N}{R_N + Z} \\
F_{65} &= \frac{\partial f_6}{\partial v_E} = -2\Omega \cos L - \frac{2v_E}{R_E + Z} \\
F_{67} &= \frac{\partial f_6}{\partial \phi} = \frac{\partial C_{31}}{\partial \phi} f_x + \frac{\partial C_{32}}{\partial \phi} f_y + \frac{\partial C_{33}}{\partial \phi} f_z \\
F_{68} &= \frac{\partial f_6}{\partial \theta} = \frac{\partial C_{31}}{\partial \theta} f_x + \frac{\partial C_{32}}{\partial \theta} f_y + \frac{\partial C_{33}}{\partial \theta} f_z \\
F_{69} &= \frac{\partial f_6}{\partial \psi} = \frac{\partial C_{31}}{\partial \psi} f_x + \frac{\partial C_{32}}{\partial \psi} f_y + \frac{\partial C_{33}}{\partial \psi} f_z \\
F_{71} &= \frac{\partial f_7}{\partial L} = \left(\frac{\partial \omega_y}{\partial L} \sin \phi + \frac{\partial \omega_z}{\partial L} \cos \phi \right) \tan \theta \\
&\quad + \frac{\partial \omega_x}{\partial L} \\
F_{73} &= \frac{\partial f_7}{\partial Z} = \left(\frac{\partial \omega_y}{\partial Z} \sin \phi + \frac{\partial \omega_z}{\partial Z} \cos \phi \right) \tan \theta \\
&\quad + \frac{\partial \omega_x}{\partial Z} \\
F_{74} &= \frac{\partial f_7}{\partial v_N} = \left(\frac{\partial \omega_y}{\partial v_N} \sin \phi + \frac{\partial \omega_z}{\partial v_N} \cos \phi \right) \tan \theta \\
&\quad + \frac{\partial \omega_x}{\partial v_N} \\
F_{75} &= \frac{\partial f_7}{\partial v_E} = \left(\frac{\partial \omega_y}{\partial v_E} \sin \phi + \frac{\partial \omega_z}{\partial v_E} \cos \phi \right) \tan \theta \\
&\quad + \frac{\partial \omega_x}{\partial v_E} \\
F_{76} &= \frac{\partial f_7}{\partial v_D} = \left(\frac{\partial \omega_y}{\partial v_D} \sin \phi + \frac{\partial \omega_z}{\partial v_D} \cos \phi \right) \tan \theta \\
&\quad + \frac{\partial \omega_x}{\partial v_D} \\
F_{77} &= \frac{\partial f_7}{\partial \phi} = \left(\frac{\partial \omega_y}{\partial \phi} \sin \phi + \omega_y \cos \phi \right) \tan \theta \\
&\quad + \left(\frac{\partial \omega_z}{\partial \phi} \cos \phi - \omega_z \sin \phi \right) \tan \theta + \frac{\partial \omega_x}{\partial \phi} \\
F_{78} &= \frac{\partial f_7}{\partial \theta} = \left(\frac{\partial \omega_y}{\partial \theta} \sin \phi + \frac{\partial \omega_z}{\partial \theta} \cos \phi \right) \tan \theta \\
&\quad + (\omega_y \sin \phi + \omega_z \cos \phi) \sec^2 \theta + \frac{\partial \omega_x}{\partial \theta}
\end{aligned}$$

$$\begin{aligned}
F_{79} &= \frac{\partial f_7}{\partial \psi} = \left(\frac{\partial \omega_y}{\partial \psi} \sin \phi + \frac{\partial \omega_z}{\partial \psi} \cos \phi \right) \tan \theta + \frac{\partial \omega_x}{\partial \psi} \\
F_{81} &= \frac{\partial f_8}{\partial L} = \left(\frac{\partial \omega_y}{\partial L} \cos \phi - \frac{\partial \omega_z}{\partial L} \sin \phi \right) \\
F_{83} &= \frac{\partial f_8}{\partial Z} = \left(\frac{\partial \omega_y}{\partial Z} \cos \phi - \frac{\partial \omega_z}{\partial Z} \sin \phi \right) \\
F_{84} &= \frac{\partial f_8}{\partial v_N} = \left(\frac{\partial \omega_y}{\partial v_N} \cos \phi - \frac{\partial \omega_z}{\partial v_N} \sin \phi \right) \\
F_{85} &= \frac{\partial f_8}{\partial v_E} = \left(\frac{\partial \omega_y}{\partial v_E} \cos \phi - \frac{\partial \omega_z}{\partial v_E} \sin \phi \right) \\
F_{86} &= \frac{\partial f_8}{\partial v_D} = \left(\frac{\partial \omega_y}{\partial v_D} \cos \phi - \frac{\partial \omega_z}{\partial v_D} \sin \phi \right) \\
F_{87} &= \frac{\partial f_8}{\partial \phi} = \left(\frac{\partial \omega_y}{\partial \phi} \cos \phi - \omega_y \sin \phi \right) \\
&\quad - \left(\frac{\partial \omega_z}{\partial \phi} \sin \phi + \omega_z \cos \phi \right) \\
F_{88} &= \frac{\partial f_8}{\partial \theta} = \left(\frac{\partial \omega_y}{\partial \theta} \cos \phi - \frac{\partial \omega_z}{\partial \theta} \sin \phi \right) \\
F_{89} &= \frac{\partial f_8}{\partial \psi} = \left(\frac{\partial \omega_y}{\partial \psi} \cos \phi - \frac{\partial \omega_z}{\partial \psi} \sin \phi \right) \\
F_{91} &= \frac{\partial f_9}{\partial L} = \left(\frac{\partial \omega_y}{\partial L} \sin \phi + \frac{\partial \omega_z}{\partial L} \cos \phi \right) \sec \theta \\
F_{93} &= \frac{\partial f_9}{\partial Z} = \left(\frac{\partial \omega_y}{\partial Z} \sin \phi + \frac{\partial \omega_z}{\partial Z} \cos \phi \right) \sec \theta \\
F_{94} &= \frac{\partial f_9}{\partial v_N} = \left(\frac{\partial \omega_y}{\partial v_N} \sin \phi + \frac{\partial \omega_z}{\partial v_N} \cos \phi \right) \sec \theta \\
F_{95} &= \frac{\partial f_9}{\partial v_E} = \left(\frac{\partial \omega_y}{\partial v_E} \sin \phi + \frac{\partial \omega_z}{\partial v_E} \cos \phi \right) \sec \theta \\
F_{96} &= \frac{\partial f_9}{\partial v_D} = \left(\frac{\partial \omega_y}{\partial v_D} \sin \phi + \frac{\partial \omega_z}{\partial v_D} \cos \phi \right) \sec \theta \\
F_{97} &= \frac{\partial f_9}{\partial \phi} = \left(\frac{\partial \omega_y}{\partial \phi} \sin \phi + \omega_y \cos \phi \right) \sec \theta \\
&\quad + \left(\frac{\partial \omega_z}{\partial \phi} \cos \phi - \omega_z \sin \phi \right) \sec \theta \\
F_{98} &= \frac{\partial f_9}{\partial \theta} = \left(\frac{\partial \omega_y}{\partial \theta} \sin \phi + \frac{\partial \omega_z}{\partial \theta} \cos \phi \right) \sec \theta \\
&\quad + (\omega_y \sin \phi + \omega_z \cos \phi) \sec \theta \tan \theta \\
F_{99} &= \frac{\partial f_9}{\partial \psi} = \left(\frac{\partial \omega_y}{\partial \psi} \sin \phi + \frac{\partial \omega_z}{\partial \psi} \cos \phi \right) \sec \theta
\end{aligned}$$

where the following derivatives can be calculated

$$\frac{\partial R_N}{\partial L} = \frac{3}{2} e^2 \sin(2L) R (1 - e^2) (1 - e^2 \sin^2 L)^{-\frac{5}{2}}$$

$$\begin{aligned}
\frac{\partial R_E}{\partial L} &= \frac{1}{2} e^2 \sin(2L) R (1 - e^2 \sin^2 L)^{-\frac{3}{2}} \\
\frac{\partial C_{11}}{\partial \phi} &= 0 \\
\frac{\partial C_{12}}{\partial \phi} &= \sin \phi \sin \psi + \cos \phi \sin \theta \cos \psi \\
\frac{\partial C_{13}}{\partial \phi} &= \cos \phi \sin \psi - \sin \phi \sin \theta \cos \psi \\
\frac{\partial C_{11}}{\partial \theta} &= -\sin \theta \cos \psi \\
\frac{\partial C_{12}}{\partial \theta} &= \sin \phi \cos \theta \cos \psi \\
\frac{\partial C_{13}}{\partial \theta} &= \cos \phi \cos \theta \cos \psi \\
\frac{\partial C_{11}}{\partial \psi} &= -\cos \theta \sin \psi \\
\frac{\partial C_{12}}{\partial \psi} &= -\cos \phi \cos \psi - \sin \phi \sin \theta \sin \psi \\
\frac{\partial C_{13}}{\partial \psi} &= \sin \phi \cos \psi - \cos \phi \sin \theta \sin \psi \\
\frac{\partial C_{21}}{\partial \phi} &= 0 \\
\frac{\partial C_{22}}{\partial \phi} &= -\sin \phi \cos \psi + \cos \phi \sin \theta \sin \psi \\
\frac{\partial C_{23}}{\partial \phi} &= -\cos \phi \cos \psi - \sin \phi \sin \theta \sin \psi \\
\frac{\partial C_{21}}{\partial \theta} &= -\sin \theta \sin \psi \\
\frac{\partial C_{22}}{\partial \theta} &= \sin \phi \cos \theta \sin \psi \\
\frac{\partial C_{23}}{\partial \theta} &= \cos \phi \cos \theta \sin \psi \\
\frac{\partial C_{21}}{\partial \psi} &= \cos \theta \cos \psi \\
\frac{\partial C_{22}}{\partial \psi} &= -\cos \phi \sin \psi + \sin \phi \sin \theta \cos \psi \\
\frac{\partial C_{23}}{\partial \psi} &= \sin \phi \sin \psi + \cos \phi \sin \theta \cos \psi \\
\frac{\partial C_{31}}{\partial \phi} &= 0 \\
\frac{\partial C_{32}}{\partial \phi} &= \cos \phi \cos \theta \\
\frac{\partial C_{33}}{\partial \phi} &= -\sin \phi \cos \theta \\
\frac{\partial C_{31}}{\partial \theta} &= -\cos \theta
\end{aligned}$$

$$\begin{aligned}
\frac{\partial C_{32}}{\partial \theta} &= -\sin \phi \sin \theta \\
\frac{\partial C_{33}}{\partial \theta} &= -\cos \phi \sin \theta \\
\frac{\partial C_{31}}{\partial \psi} &= \frac{\partial C_{32}}{\partial \psi} = \frac{\partial C_{33}}{\partial \psi} = 0 \\
\frac{\partial \omega_x}{\partial L} &= -\left(C_{11} \frac{\partial \omega_N}{\partial L} + C_{21} \frac{\partial \omega_E}{\partial L} + C_{31} \frac{\partial \omega_D}{\partial L} \right) \\
\frac{\partial \omega_x}{\partial l} &= 0 \\
\frac{\partial \omega_x}{\partial Z} &= -\left(C_{11} \frac{\partial \omega_N}{\partial Z} + C_{21} \frac{\partial \omega_E}{\partial Z} + C_{31} \frac{\partial \omega_D}{\partial Z} \right) \\
\frac{\partial \omega_x}{\partial v_N} &= \left(C_{21} \frac{\partial \omega_E}{\partial v_N} \right) \\
\frac{\partial \omega_x}{\partial v_E} &= -\left(C_{11} \frac{\partial \omega_N}{\partial v_E} + C_{31} \frac{\partial \omega_D}{\partial v_E} \right) \\
\frac{\partial \omega_x}{\partial v_D} &= 0 \\
\frac{\partial \omega_x}{\partial \phi} &= -\left(C_{11} \frac{\partial \omega_N}{\partial \phi} + C_{21} \frac{\partial \omega_E}{\partial \phi} + C_{31} \frac{\partial \omega_D}{\partial \phi} \right) \\
\frac{\partial \omega_x}{\partial \theta} &= -\left(C_{11} \frac{\partial \omega_N}{\partial \theta} + C_{21} \frac{\partial \omega_E}{\partial \theta} + C_{31} \frac{\partial \omega_D}{\partial \theta} \right) \\
\frac{\partial \omega_x}{\partial \psi} &= -\left(C_{11} \frac{\partial \omega_N}{\partial \psi} + C_{21} \frac{\partial \omega_E}{\partial \psi} + C_{31} \frac{\partial \omega_D}{\partial \psi} \right) \\
\frac{\partial \omega_y}{\partial L} &= -\left(C_{12} \frac{\partial \omega_N}{\partial L} + C_{22} \frac{\partial \omega_E}{\partial L} + C_{32} \frac{\partial \omega_D}{\partial L} \right) \\
\frac{\partial \omega_y}{\partial l} &= 0 \\
\frac{\partial \omega_y}{\partial Z} &= -\left(C_{12} \frac{\partial \omega_N}{\partial Z} + C_{22} \frac{\partial \omega_E}{\partial Z} + C_{32} \frac{\partial \omega_D}{\partial Z} \right) \\
\frac{\partial \omega_y}{\partial v_N} &= \left(C_{22} \frac{\partial \omega_E}{\partial v_N} \right) \\
\frac{\partial \omega_y}{\partial v_E} &= -\left(C_{12} \frac{\partial \omega_N}{\partial v_E} + C_{32} \frac{\partial \omega_D}{\partial v_E} \right) \\
\frac{\partial \omega_y}{\partial v_D} &= 0 \\
\frac{\partial \omega_y}{\partial \phi} &= -\left(C_{12} \frac{\partial \omega_N}{\partial \phi} + C_{22} \frac{\partial \omega_E}{\partial \phi} + C_{32} \frac{\partial \omega_D}{\partial \phi} \right) \\
\frac{\partial \omega_y}{\partial \theta} &= -\left(C_{12} \frac{\partial \omega_N}{\partial \theta} + C_{22} \frac{\partial \omega_E}{\partial \theta} + C_{32} \frac{\partial \omega_D}{\partial \theta} \right) \\
\frac{\partial \omega_y}{\partial \psi} &= -\left(C_{12} \frac{\partial \omega_N}{\partial \psi} + C_{22} \frac{\partial \omega_E}{\partial \psi} + C_{32} \frac{\partial \omega_D}{\partial \psi} \right) \\
\frac{\partial \omega_x}{\partial L} &= -\left(C_{13} \frac{\partial \omega_N}{\partial L} + C_{23} \frac{\partial \omega_E}{\partial L} + C_{33} \frac{\partial \omega_D}{\partial L} \right)
\end{aligned}$$

$$\begin{aligned}\frac{\partial \omega_x}{\partial l} &= 0 \\ \frac{\partial \omega_x}{\partial Z} &= - \left(C_{13} \frac{\partial \omega_N}{\partial Z} + C_{23} \frac{\partial \omega_E}{\partial Z} + C_{33} \frac{\partial \omega_D}{\partial Z} \right) \\ \frac{\partial \omega_x}{\partial v_N} &= \left(C_{23} \frac{\partial \omega_E}{\partial v_N} \right) \\ \frac{\partial \omega_x}{\partial v_E} &= - \left(C_{13} \frac{\partial \omega_N}{\partial v_E} + C_{33} \frac{\partial \omega_D}{\partial v_E} \right)\end{aligned}$$

$$\begin{aligned}\frac{\partial \omega_x}{\partial v_D} &= 0 \\ \frac{\partial \omega_x}{\partial \phi} &= - \left(C_{13} \frac{\partial \omega_N}{\partial \phi} + C_{23} \frac{\partial \omega_E}{\partial \phi} + C_{33} \frac{\partial \omega_D}{\partial \phi} \right) \\ \frac{\partial \omega_x}{\partial \theta} &= - \left(C_{13} \frac{\partial \omega_N}{\partial \theta} + C_{23} \frac{\partial \omega_E}{\partial \theta} + C_{33} \frac{\partial \omega_D}{\partial \theta} \right) \\ \frac{\partial \omega_x}{\partial \psi} &= - \left(C_{13} \frac{\partial \omega_N}{\partial \psi} + C_{23} \frac{\partial \omega_E}{\partial \psi} + C_{33} \frac{\partial \omega_D}{\partial \psi} \right) \\ \frac{\partial \omega_N}{\partial L} &= -\Omega \sin L - \frac{\partial R_E}{\partial L} \frac{v_E}{(R_E + Z)^2} \\ \frac{\partial \omega_N}{\partial Z} &= - \frac{v_E}{(R_E + Z)^2} \\ \frac{\partial \omega_E}{\partial L} &= - \frac{\partial R_N}{\partial L} \frac{v_N}{(R_E + Z)^2} \\ \frac{\partial \omega_E}{\partial Z} &= \frac{v_N}{(R_N + Z)^2} \\ \frac{\partial \omega_E}{\partial v_N} &= - \frac{1}{R_N + Z} \\ \frac{\partial \omega_D}{\partial L} &= -\Omega \cos L + \frac{\partial R_E}{\partial L} \frac{v_E \tan L}{(R_E + Z)^2} - \frac{v_E \sec^2 L}{R_E + Z} \\ \frac{\partial \omega_D}{\partial Z} &= \frac{v_E \tan L}{(R_E + Z)^2} \\ \frac{\partial \omega_D}{\partial v_E} &= \frac{-\tan L}{R_E + Z}\end{aligned}$$

Taking derivatives of v_x , v_y , and v_z with respect to the orientation states gives

$$\begin{aligned}H_{17} &= \frac{\partial v_x}{\partial \phi} = \frac{\partial C_{11}}{\partial \phi} v_N + \frac{\partial C_{21}}{\partial \phi} v_E + \frac{\partial C_{31}}{\partial \phi} v_D \\ H_{18} &= \frac{\partial v_x}{\partial \theta} = \frac{\partial C_{11}}{\partial \theta} v_N + \frac{\partial C_{21}}{\partial \theta} v_E + \frac{\partial C_{31}}{\partial \theta} v_D \\ H_{19} &= \frac{\partial v_x}{\partial \psi} = \frac{\partial C_{11}}{\partial \psi} v_N + \frac{\partial C_{21}}{\partial \psi} v_E + \frac{\partial C_{31}}{\partial \psi} v_D \\ H_{27} &= \frac{\partial v_y}{\partial \phi} = \frac{\partial C_{12}}{\partial \phi} v_N + \frac{\partial C_{22}}{\partial \phi} v_E + \frac{\partial C_{32}}{\partial \phi} v_D \\ H_{28} &= \frac{\partial v_y}{\partial \theta} = \frac{\partial C_{12}}{\partial \theta} v_N + \frac{\partial C_{22}}{\partial \theta} v_E + \frac{\partial C_{32}}{\partial \theta} v_D\end{aligned}$$

$$\begin{aligned}H_{29} &= \frac{\partial v_y}{\partial \psi} = \frac{\partial C_{12}}{\partial \psi} v_N + \frac{\partial C_{22}}{\partial \psi} v_E + \frac{\partial C_{32}}{\partial \psi} v_D \\ H_{37} &= \frac{\partial v_z}{\partial \phi} = \frac{\partial C_{13}}{\partial \phi} v_N + \frac{\partial C_{23}}{\partial \phi} v_E + \frac{\partial C_{33}}{\partial \phi} v_D \\ H_{38} &= \frac{\partial v_z}{\partial \theta} = \frac{\partial C_{13}}{\partial \theta} v_N + \frac{\partial C_{23}}{\partial \theta} v_E + \frac{\partial C_{33}}{\partial \theta} v_D \\ H_{39} &= \frac{\partial v_z}{\partial \psi} = \frac{\partial C_{13}}{\partial \psi} v_N + \frac{\partial C_{23}}{\partial \psi} v_E + \frac{\partial C_{33}}{\partial \psi} v_D\end{aligned}$$

References

1. Brokloff, N.: Dead reckoning with an adcp and current extrapolation. In: IEEE/MTS OCEANS, vol. 2, pp. 994–100. Halifax, NS, Canada (October 1997)
2. Groves, P.D.: Principles of GNSS, Inertial, and Multisensor Integrated Navigation Systems. Artech House, Boston (2008)
3. Park, M., Gao, Y.: Error analysis and stochastic modeling of low-cost mems accelerometer. J. Intell. Robot. Syst. **46**(1), 27–41 (2006)
4. Farrell, J.A.: Aided Navigation GPS with High Rate Sensors. McGraw-Hill Professional, New York (2008)
5. RD Instruments: ADCP Coordinate Transformation, Formulas and Calculations. San Diego, RD Instruments (1998)
6. Jalving, B., Gade, K., Hagen, O.K.: A toolbox of aiding techniques for the hugin auv integrated inertial navigation system. In: Oceans 2003 MTS/IEEE, San Diego, CA (September 2003)
7. Pitman, G.R.: Inertial Guidance. Wiley, New York (1962)
8. Britting, K.R.: Inertial Navigation Systems Analysis. Wiley, New York (1971)
9. Ali, J., Ullah, R., Mirza, M.B.: Performance comparison among some nonlinear lters for a low cost sins/gps integrated solution. Nonlinear Dyn. **61**(3), 491–502 (2010)
10. Jwo, D.J., Yang, C.F., Chuang, C.H., Lee, T.Y.: Performance enhancement for ultra-tight gps/ins integration using a fuzzy adaptive strong tracking unscented kalman lter. Nonlinear Dyn. **73**(1–2), 377–395 (2013)
11. Ali, J., Ushaq, M., Majeed, S.: Robust aspects in dependable lter design for alignment of a submarine inertial navigation system. J. Mar. Sci. Technol. **17**(3), 340–348 (2012)
12. Yun, X., Bachmann, E.R., McGhee, R.B., Whalen, R.H.: Testing and evaluation of an integrated gps/ins system for small auv navigation. IEEE J. Ocean. Eng. **24**(3), 396–404 (1999)
13. Larsen, M.: High performance doppler-inertial navigation—experimental results. In: Proceedings of OCEANS 2000 MTS/IEEE, Rhode Island Convention Center (September 2000)
14. McEwen, R., Thomas, H., Weber, D., Psota, F.: Performance of an AUV navigation system at arctic latitudes. IEEE J. Ocean. Eng. **30**(2), 443–454 (2005)
15. Kussat, N.H., Chadwell, C.D., Zimmerman, R.: Absolute positioning of an autonomous underwater vehicle using gps and acoustic measurements. IEEE J. Ocean. Eng. **30**(1), 153–164 (2005)

16. Kinsey, J.C., Eustice, R.M., Whitcomb, L.L.: A survey of underwater vehicle navigation: Recent advances and new challenges. In: IFAC Conference on Maneuvering and Control of Marine Craft, Lisbon, Portugal (September 2006)
17. Lee, P.M., Jun, B.H., Kim, K., Lee, J., Aoki, T., Hyakudome, T.: Simulation of an inertial acoustic navigation system with range aiding for an autonomous underwater vehicle. *IEEE J. Ocean. Eng.* **32**(2), 327–345 (2007)
18. Miller, P.A., Farrell, J.A., Zhao, Y., Djapic, V.: Autonomous underwater vehicle navigation. *IEEE J. Ocean. Eng.* **35**(3), 663–678 (2010)
19. Vasilijevic, A., Borovic, B., Vukic, Z.: Underwater vehicle localization with complementary filter: performance analysis in the shallow water environment. *J. Intell. Robot. Syst.* **68**(3–4), 373–386 (2012)
20. Grenon, G., An, P.E., Smith, S.M., Healey, A.J.: Enhancement of the inertial navigation system for the morpheus autonomous underwater vehicles. *IEEE J. Ocean. Eng.* **26**(4), 548–560 (2001)
21. Marco, D.B., Healey, A.J.: Command, control, and navigation experimental results with the NPS ARIES AUV. *IEEE J. Ocean. Eng.* **26**(4), 466–476 (2001)
22. Lee, P.M., Jun, B.H.: Pseudo long base line navigation algorithm for underwater vehicles with inertial sensors and two acoustic range measurement. *Ocean Eng.* **34**(3), 416–425 (2006)
23. Stutters, L., Liu, H., Tiltman, C., Brown, D.J.: Navigation technologies for autonomous underwater vehicles. *IEEE Trans. Syst. Man Cybern.* **38**(4), 581–589 (2008)
24. Grewal, M.S., Andrews, A.P.: *Kalman Filtering Theory and Practice Using MATLAB*, 3rd edn. Wiley, New Jersey (2008)
25. Brown, R.G., Hwang, P.Y.C.: *Introduction to Random Signals and Applied Kalman Filtering*. Wiley, New York (1997)
26. Bar-Shalom, Y., Lee, X.R., Kirubarajan, T.: *Estimation with Applications To Tracking and Navigation*. Wiley, New York (2001)
27. Kalman, R.E.: A new approach to linear filtering and prediction problems. *ASME Trans. Ser. D: J. Basic Eng.* **82**(1), 34–45 (1960)
28. Majji, M., Junkins, J.L., Turner, J.D.: A perturbation method for estimation of dynamic systems. *Nonlinear Dyn.* **60**(3), 303–325 (2010)
29. Maybeck, P.S.: *Stochastic models, estimation, and control*, vol. 1. Academic Press, New York (1979)
30. Farrell, J.A., Barth, M.: *The Global Positioning System and Inertial Navigation*. McGraw-Hill Professional, New York (1999)
31. Qi, H., Moore, J.B.: Direct Kalman filtering approach for GPS/INS integration. *IEEE Trans. Aerosp. Electron. Syst.* **38**(2), 687–693 (2002)
32. Wendel, J., Schlaile, C., Trommer, G.F.: Direct Kalman filtering of GPS/INS for aerospace applications. In: *International Symposium on Kinematic System in Geodesy, Geomatics and Navigation*, Alberta, Canada (2001)
33. Zhao, L., Gao, W.: The experimental study on gps/ins/dvl integration for auv. In: *Proceedings of the Position Location Navigation Symposium, PLANS 2004*. pp. 337–340 (April 2004)
34. Jo, G., Choi, H.S.: Velocity-aided underwater navigation system using receding horizon Kalman filter. *IEEE J. Ocean. Eng.* **31**(3), 565–573 (2006)
35. Hegrens, O., Hallingstad, O.: Model-aided INS with sea current estimation for robust underwater navigation. *IEEE J. Ocean. Eng.* **36**(2), 316–337 (2011)
36. Titterton, D.H., Weston, J.L.: *Strapdown Inertial Navigation Technology*. The Institution of Electrical Engineers, UK (2004)
37. Simon, D.: *Optimal State Estimation Kalman, H ∞ and Nonlinear Approaches*. Wiley, New Jersey (2006)
38. Mariani, S., Ghisi, A.: Unscented kalman ltering for nonlinear structural dynamics. *Nonlinear Dyn.* **49**(1–2), 131–150 (2007)
39. Shabani, M., Gholami, A., Davari, N., Emami, M.: Implementation and performance comparison of indirect kalman filtering approaches for AUV integrated navigation system using low cost IMU. In: *ICEE2013, Mashhad, Iran*, pp. 1–6 (May 2013)